Available online at www.sciencedirect.com
SCIENCE DIRECT®
Geochimica et Cosmochimica Acta 70 (2006) 533–547
Geochimica
www.elsevier.com/locate/gca

Kinetics of sorption and abiotic oxidation of arsenic(III) by aquifer materials

Aria Amirbahman [a,*], Douglas B. Kent [b], Gary P. Curtis [b], James A. Davis [b]

[a] Department of Civil and Environmental Engineering, University of Maine, Orono, ME 04469, USA
[b] US Geological Survey, 345 Middlefield Rd., Menlo Park, CA 94025, USA

Received 16 May 2005; accepted in revised form 4 October 2005

Abstract

The fate of arsenic in groundwater depends largely on its interaction with mineral surfaces. We investigated the kinetics of As(III) oxidation by aquifer materials collected from the USGS research site at Cape Cod, MA, USA, by conducting laboratory experiments. Five different solid samples with similar specific surface areas (0.6–0.9 $m^2\ g^{-1}$) and reductively extractable iron contents (18–26 $\mu mol\ m^{-2}$), but with varying total manganese contents (0.5–3.5 $\mu mol\ m^{-2}$) were used. Both dissolved and adsorbed As(III) and As(V) concentrations were measured with time up to 250 h. The As(III) removal rate from solution increased with increasing solid manganese content, suggesting that manganese oxide is responsible for the oxidation of As(III). Under all conditions, dissolved As(V) concentrations were very low. A quantitative model was developed to simulate the extent and kinetics of arsenic transformation by aquifer materials. The model included: (1) reversible rate-limited adsorption of As(III) onto both oxidative and non-oxidative (adsorptive) sites, (2) irreversible rate-limited oxidation of As(III), and (3) equilibrium adsorption of As(V) onto adsorptive sites. Rate constants for these processes, as well as the total oxidative site densities were used as the fitting parameters. The total adsorptive site densities were estimated based on the measured specific surface area of each material. The best fit was provided by considering one fast and one slow site for each adsorptive and oxidative site. The fitting parameters were obtained using the kinetic data for the most reactive aquifer material at different initial As(III) concentrations. Using the same parameters to simulate As(III) and As(V) surface reactions, the model predictions were compared to observations for aquifer materials with different manganese contents. The model simulated the experimental data very well for all materials at all initial As(III) concentrations. The As(V) production rate was related to the concentrations of the free oxidative surface sites and dissolved As(III), as $r_{As(V)} = k'_{ox}[\rangle Mn^{(IV)}OH][H_3AsO_3]$ with apparent second-order rate constants of $k^{f'}_{ox} = 6.28 \times 10^{-1}$ and $k^{s'}_{ox} = 1.25 \times 10^{-2}\ M^{-1}\ s^{-1}$ for the fast and the slow oxidative sites, respectively. The As(III) removal rate decreased approximately by half for a pH increase from 4 to 7. The pH dependence was explained using the acid–base behavior of the surface oxidative sites by considering a surface $pK_a = 6.2$ ($I = 0$). In the presence of excess surface adsorptive and oxidative sites, phosphate diminished the rate of As(III) removal and As(V) production only slightly due to its interaction with the oxidative sites. The observed As(III) oxidation rate here is consistent with previous observations of As(III) oxidation over short transport distances during field-scale transport experiments. The model developed here may be incorporated into groundwater transport models to predict arsenic speciation and transport in chemically heterogeneous systems.

1. Introduction

Arsenic contamination of drinking water is an issue of great concern. Due to its acute toxicity to humans, the World Health Organization (WHO) has set a maximum contaminant level (MCL) of 10 $\mu g\ L^{-1}$ for arsenic in drinking water (WHO, 1993). Depending on its source, arsenic concentrations in natural waters may range up to several hundred milligrams per liter. Arsenic contamination of groundwater has been of great interest in several countries, most notably in Bangladesh and West Bengal, where two-thirds of the population are at risk of serious health effects due to high concentrations of arsenic in the shallow alluvial

* Corresponding author. Fax: +1 207 581 3888.
E-mail address: aria@umit.maine.edu (A. Amirbahman).

0016-7037/$ - see front matter © 2005 Elsevier Inc. All rights reserved.
doi:10.1016/j.gca.2005.10.036

and deltaic aquifers that are the main sources of drinking water (Manzurul Hassan et al., 2003).

Mobilization of sediment-bound arsenic in natural and contaminated groundwater has been observed under a variety of chemical conditions (Smedley and Kinniburgh, 2002). Increasing arsenic mobility in groundwater in response to elevated pH values (>10) has been reported (Mariner et al., 1996). In oxic environments, release of sediment-bound arsenic has been observed in response to elevated concentrations of phosphate (Kent and Fox, 2004) and oxidation of sulfide minerals at low pH values (McCreadie et al., 2000; Schreiber et al., 2000). In anoxic environments, sediment-bound arsenic can be mobilized by reductive dissolution or transformation of Fe(III) hydroxide coatings and reduction of arsenate (As(V)) to arsenite (As(III)) (e.g., Belzile and Tessier, 1990; Ahmann et al., 1997; Harrington et al., 1998; Cummings et al., 1999; McArthur et al., 2001; Höhn et al., 2001; Harvey et al., 2002; Horneman et al., 2004; Kent and Fox, 2004; Swartz et al., 2004; van Geen et al., 2004).

Speciation of arsenic controls its mobility and toxicity in natural waters. In most natural waters, arsenic speciation is dominated by the oxyanions As(III) and As(V) (Smedley and Kinniburgh, 2002). In general, As(V) adsorption to mineral oxides is favored at low pH, whereas maximum As(III) adsorption occurs at circumneutral pH and decreases with an increase or a decrease in pH (Raven et al., 1998; Arai et al., 2001; Dixit and Hering, 2003). As(III), however, is known to be more toxic than As(V) to humans (National Research Council, 1999). Therefore, understanding the redox speciation of inorganic arsenic involving As(III) and As(V) species is of great importance.

Both biotic and abiotic processes can lead to redox transformation of arsenic species. Several microbial respiratory and non-respiratory enzymatic systems for oxidation of As(III) have been reported (Oremland and Stolz, 2003). In natural systems, the most important abiotic pathway for the oxidation of As(III) is by minerals containing Mn(III) and Mn(IV) (Oscarson et al., 1981a,b; Brannon and Patrick, 1987). Experimental studies using synthetic and biogenic manganese oxides have shown that these solids can effectively oxidize As(III), albeit at different rates that span an order of magnitude (Oscarson et al., 1983; Moore and Walker, 1990; Scott and Morgan, 1995; Chui and Hering, 2000; Tournassat et al., 2002; Tani et al., 2004). Tournassat et al. (2002) attributed differences in As(III) oxidation rate to the degree of crystallinity and structure of manganese minerals. An experimental study on sediment samples showed that removal of manganese oxides resulted in a marked decrease in the As(III) oxidation rate (Oscarson et al., 1981a).

Previous studies of As(III) oxidation kinetics by synthetic manganese oxides show that the kinetics of aqueous As(III) removal do not display a simple first-order behavior (Moore et al., 1990; Scott and Morgan, 1995; Chui and Hering, 2000; Manning et al., 2002; Tournassat et al., 2002). As(III) oxidation by manganese oxides involves a series of steps, including diffusion of As(III) to oxidative sites, ligand exchange between As(III) and manganese oxide surface functional groups, and inner-sphere electron transfer. Alternatively, outer-sphere electron transfer may occur between oxidative sites and As(III) through their respective coordination sheaths. The predominantly Mn(III) oxide manganite (γ-MnOOH) has been shown to oxidize As(III) and to adsorb both As(III) and As(V) species (Chui and Hering, 2000). Adsorption of As(III) onto manganese oxides consisting predominantly of Mn(IV) has not been observed. Adsorption of As(V) onto manganese(IV) oxides, however, has been reported (e.g., Tani et al., 2004), and spectroscopic studies have shown that the structure of the As(V) surface complex on manganese oxides is similar to that on Fe(III) hydroxides (Manning et al., 2002; Deschamps et al., 2003; Foster et al., 2003).

In the presence of natural composite surfaces, both oxidation and adsorption reactions should be considered for the removal of arsenic from solution. The Fe(III)- and Al-bearing minerals in natural soil and sediment surfaces adsorb arsenic (Pierce and Moore, 1980; Fuller et al., 1993; Manning and Goldberg, 1996; Wilkie and Hering, 1996; Fendorf et al., 1997; Raven et al., 1998; Dixit and Hering, 2003; Arai et al., 2005). Arsenic, however, has a higher affinity to Fe(III) hydroxides than to Al hydroxides and clay minerals (Manning and Goldberg, 1997;Arai et al., 2001). Adsorption of arsenic species onto Fe(III) hydroxides is pH-dependent. At acidic pH, As(V) generally sorbs more favorably than As(III), whereas at basic pH, the trend is reversed (Manning et al., 1998; Raven et al., 1998; Dixit and Hering, 2003). The pH behavior of As(III) adsorption onto Fe(III) hydroxides, however, shows a smaller pH dependency than that of As(V). The exact pH adsorption behavior may be attributed to the acid–base characteristics of aqueous As(V) and As(III), and acid–base characteristics and adsorption affinity of surface functional groups on the solids (Davis and Kent, 1990; Dzombak and Morel, 1990). Competitive or cooperative effects induced by the presence of other adsorbing anions or cations can significantly influence the adsorption and mobility of As(III) and As(V) (Wilkie and Hering, 1996; Darland and Inskeep, 1997; Gräfe et al., 2004; Kent and Fox, 2004).

Over short timescales, as might be encountered in laboratory experiments and some surface- and groundwater applications, arsenic interaction with mineral surfaces may be controlled kinetically (Johnson and Pilson, 1975; Seyler and Martin, 1989; Kuhn and Sigg, 1993). In batch laboratory experiments, arsenic adsorption kinetics onto Fe(III) hydroxides have been shown to be relatively fast, with a faster rate observed for As(V) at lower pH values, and for As(III) at higher pH values (Raven et al., 1998; Waltham and Eick, 2002). The extent and kinetics of As(V) and As(III) adsorption onto Fe(III) hydroxides were shown to be dependent on the solute:sorbent ratio (Pierce and Moore, 1980; Raven et al., 1998).

The above-mentioned studies have investigated arsenic interactions with synthetic and, in a few cases, naturally occurring manganese oxides. However, studies that model arsenic interaction kinetics with natural composite materials are lacking. In this work, we have conducted batch experiments to examine the adsorption and oxidation of As(III) by aquifer materials from five different locations at the USGS research site on Cape Cod, MA, USA (LeBlanc, 1984; LeBlanc et al., 1991; Kent et al., 1995; Kent and Fox, 2004). The aquifer is shallow and unconfined, and its mineralogy is dominated by quartz, feldspars, and other silicate minerals. These materials contain relatively similar specific surface areas and reductively extractable iron contents. However, they differ greatly in the reductively extractable manganese contents. The objective of this paper is to develop a macroscopic kinetic model based on the laws of surface complexation and mass-action that accounts for uptake of arsenic by adsorption and oxidation in the presence of aquifer materials from the Cape Cod site. This model involves a multi-step reaction scheme involving adsorption of As(III) onto oxidative and adsorptive sites on the aquifer material, electron transfer at the oxidative sites followed by As(V) release, and the reaction of As(V) with the adsorptive sites. The model developed here is calibrated using experimental data with aquifer materials under varying chemical conditions and may be used to simulate the major features of reactive transport of arsenic in chemically heterogeneous groundwater systems.

2. Experimental section

2.1. Materials

Aquifer materials from five different locations in the USGS groundwater experiment site in Cape Cod, MA (USA) were used (Table 1). All solid samples were obtained from a region of the aquifer that was oxic (250–350 μM dissolved oxygen), had low concentrations of dissolved salts (specific conductance $<100\ \mu S\ cm^{-1}$), and acidic pH values (4.8–5.8) at locations described in detail elsewhere. Sample F415-19 was obtained adjacent to a site previously designated the "suboxic" site (Kent et al., 1994). Sample R23AW was a composite of materials obtained from 2 cores (R23AWC02 and C03) adjacent to a site where arsenic tracer tests had been conducted (Stadler et al., 2001; Kent and Fox, 2004). Samples F168 were obtained approximately 2 km downgradient at a site previously designated the "oxic" site (Kent et al., 1995). These materials consist of approximately 90% quartz with the remainder as plagioclase and K-feldspars, magnetite, hematite, goethite, glauconite, and lithic fragments (Barber, 1990; Wood et al., 1990; Bau et al., 2004). The surfaces of quartz and other mineral grains are, however, coated with nm-size Fe(III)- and Al-hydroxides and/or silicates (Coston et al., 1995; Banfield and Hamers, 1997). Aquifer materials were collected using a wire-line core barrel (Zapico et al., 1987) and frozen. They were air-dried, sieved to remove material greater than 2 mm in diameter, and stored dry until use.

All chemicals used in this study were reagent grade. A 0.05 M concentration stock solution of As(III) was prepared in an anaerobic glove bag by dissolving $NaAsO_2$ salt (Baker) (brand names are for identification purposes only and should not be taken to construe endorsement by the US Geological Survey) in an oxygen-free 0.01 M solution of HCl. This solution was stored in a Teflon bottle in the dark in an anaerobic glove bag. A 0.05 M concentration of As(V) stock solution was prepared by dissolving $Na_2HAsO_4{\cdot}7H_2O$ salt (Baker) in a 0.01 M solution of HCl. This solution was stored in a Teflon bottle in the dark. A 2 M stock solution of NaCl (Aldrich) was used to adjust the background ionic strength of the samples. The buffer solutions of sodium acetate (Baker) and 2,2-bis(hydroxymethyl)-2,2′,2″-nitrilotriethanol (Bis-Tris; Aldrich) were freshly prepared before the start of each experiment. Reductive extraction of iron and manganese from the aquifer materials was performed with hydroxylamine hydrochloride ($NH_2OH{\cdot}HCl$; Aldrich). Oxalic acid, HCl, HNO_3, and NaOH were obtained from Aldrich.

2.2. Experimental setup

The As(III) oxidation experiments were conducted by adding 17.50 ± 0.05 g of dry aquifer material to a 25 ml buffer solution in 50 mL polycarbonate centrifuge tubes. The buffers were 5 mM sodium acetate (pH 5.2 and 6.0) and 5 mM Bis-Tris (pH 6.9). The ionic strength was adjusted to 10 mM by addition of NaCl. The tubes were rotated end-over-end at approximately 13 rpm in the dark for at least 16 h prior to the addition of As(III). A relatively low mixing rate was chosen to avoid excessive abrasion of the solid materials. The experiments were initiated by adding aliquots of As(III) from the stock solution to the

Table 1
Characteristics of the aquifer materials[a]

Aquifer material	Altitude (m above sea level)	Specific surface area ($m^2\ g^{-1}$)	Reductively extracted Fe content ($\mu mol\ m^{-2}$)	Reductively extracted Mn content ($\mu mol\ m^{-2}$)
F168-15	6.9 ± 0.8	0.608 ± 0.074	20.06 ± 1.05	3.36 ± 0.20
F168-20	5.3 ± 0.8	0.600 ± 0.005	22.74 ± 1.82	2.51 ± 0.23
F168-25	3.8 ± 0.8	0.845 ± 0.131	18.18 ± 3.02	1.41 ± 0.23
F415-19	13 ± 0.3	0.418 ± 0.042	26.07 ± 0.84	1.75 ± 0.14
R23AW	13.15 ± 0.45	0.531 ± 0.115	23.76 ± 1.01	0.59 ± 0.03

[a] Error is based on one standard deviation from the mean with $n = 3$.

suspensions. Initial As(III) concentrations ranging from approximately 25 to 500 μM were used. The tubes were then rotated in the dark for the duration of the experiment. Experiments were conducted both in the presence and absence of oxygen. The latter set of experiments was conducted inside an anaerobic glove bag (Coy Laboratory Products) in a N_2 atmosphere with 4% H_2. At specific times, the tubes were centrifuged and the supernatant was removed for the analysis of dissolved arsenic concentration. Kinetic experiments were continued for times longer than 150 h until steady-state conditions, especially with respect to the production of As(V), were nearly reached.

Speciation of the dissolved arsenic was determined by passing 5 mL of the supernatant followed by 5 mL of deionized water through a strong anion exchange resin (SAX; Alltech) with an exchange capacity of 0.15 meq/100 mg. The resin was conditioned prior to use with 2 mL of methanol followed by 10 mL of deionized water (Bednar et al., 2002). Under our experimental conditions, As(V) is present predominantly as $H_2AsO_4^-$ and is removed by the SAX resin, whereas As(III) is present predominantly as H_3AsO_3 and elutes through the resin column.

Solid-bound arsenic species were desorbed by adding 25 mL of 0.2 M oxalic acid after the removal of the supernatant. The tubes were then rotated in the dark for 15 min and centrifuged to remove the supernatant containing the desorbed arsenic species. Preliminary experiments showed that arsenic species were effectively desorbed using a 15 min extraction, and did not change their oxidation states, as also shown by De Vitre et al. (1991). Longer extraction times did not yield significantly higher extracted arsenic concentrations. Extraction with oxalic acid was found to be more effective and more expedient than other methods, including hot 4 M HCl and 0.02 M NaH_2EDTA.

Speciation of the adsorbed arsenic species was determined by adjusting the pH of the supernatant from the oxalic acid extract to approximately 3.8 by adding 10 M NaOH. A 1 mL solution of the extract supernatant followed by 7 mL of deionized water were then passed through the preconditioned SAX resin. As(III) concentration was determined by measuring the resin eluate, and the As(V) concentration was determined by the difference between the total arsenic concentration in the supernatant and the As(III) concentration.

2.3. Analytical methods

Arsenic was measured using inductively coupled plasma optical emission spectrometry (ICP-OES; Thermo Jarrell-Ash Iris dual-view). Prior to analysis, samples were filtered using 0.45 μm polyvinylidene fluoride filters (Millex) and acidified to pH 2 with 5 M HNO_3. Samples with high arsenic concentrations were diluted up to a 10:1 ratio. Relative precision (2 times the standard deviation divided by the average concentration determined analytically) and accuracy (ratio of the average concentration determined analytically to the known concentration) were maintained at the optimal values of 5 and 110%, respectively, by insuring arsenic concentrations exceeded the limit of quantitation of 0.13 μM, at which concentration the relative precision and accuracy greatly increased.

Approximately 5 g of each aquifer material sample was used for the N_2-BET specific surface area measurements (Micromeritics Tristar). Specific surface area determined by N_2 adsorption on this instrument was checked against a quartz sample whose specific surface area of 0.33 $m^2\ g^{-1}$ had been determined by Kr and N_2 adsorption (Kohler et al., 1996). The instrument produced reliable specific surface area values as long as the measurement was made on a sample large enough to provide at least 1 m^2 of surface area. Chemical extractions were used to determine the reductively extractable iron and manganese contents of the materials. The extractions were performed by adding the same samples used for the BET measurements to a 25 ml solution of 0.25 M $NH_2OH{\cdot}HCl$ and 0.25 M HCl. The suspension was then shaken in the dark at 50 °C for 96 h. The supernatant was filtered and diluted at a 1:1 ratio in 0.15 M HNO_3 and analyzed for iron and manganese contents. The $NH_2OH{\cdot}HCl$ extraction technique used here was found to be effective in assessing variability in adsorption properties of materials from the site (Fuller et al., 1996). Surface area measurements and extractions for all materials were performed in triplicates.

2.4. Modeling

The interactions of arsenic species with the aquifer materials described by a set of equilibrium and kinetic reactions were modeled using the computer program RATEQ (Curtis, 2005). RATEQ can simulate multiple equilibrium and rate-controlled reactions in batch systems as well as in multidimensional groundwater systems. For simultaneous equilibrium and rate-controlled reactions, RATEQ solves a set of non-linear mole-balance and mass-action equations. The code requires the user to specify the nature of the reactions (equilibrium or kinetic), the corresponding equilibrium or rate constants, total concentrations of the components, and the time intervals at which concentrations are calculated. The computer program UCODE was used to perform inverse modeling to fit a set of equilibrium and kinetic equations to the experimental data (Poeter and Hill, 1998). UCODE solves the non-linear regression problem by minimizing a weighted least squares objective function with respect to the parameter values. An estimated parameter is a quantity that appears in the input files of the application model. The parameters to be estimated in this case were the equilibrium and rate constants, and total concentrations of the surface sites. Parameter estimation is performed by running the input files of the application model, in this case several RATEQ files, simultaneously. Each of the RATEQ files contained model parameters for As(III) oxidation by one aquifer material at different initial As(III) concentrations or pH. UCODE runs the

simulations, compares the observed and simulated concentrations, and performs sensitivity calculations for each model parameter. This allows the user to observe the significance of each parameter to the simulated values, and the significance of the individual experimental observations to the estimation of the different parameters. Sensitivity analysis also aids in the identification of the most sensitive parameters. Fitting parameters with high sensitivity coefficients are estimated with a higher precision than those with low sensitivity coefficients.

3. Results and discussion

Aquifer materials from Cape Cod contain a range of reactive functional groups that originate from the mixture of mineral phases and their surface coatings (Davis et al., 1998). These coatings are primarily comprised of Fe, Al, and Si, with lesser amounts of Mn (Coston et al., 1995), likely in the form of Fe(III) hydroxides, Al hydroxides and silicates, and Mn oxides (Banfield and Hamers, 1997). Because the sediments can adsorb oxyanions (Kent et al., 1995; Stollenwerk, 1995) like As(III) and As(V), it was necessary to quantify redox speciation of arsenic in both dissolved and solid phases. This was accomplished using a 15 min extraction with oxalic acid.

3.1. Experimental results of arsenic surface interactions

Figs. 1–5 show the reaction kinetics of arsenic species at pH 5.2 at initial As(III) concentrations ranging from approximately 30 to 500 μM for the five different aquifer materials. Production of the As(V) species takes place simultaneously as the depletion of aqueous As(III) and the appearance of solid-bound As(III). Due to its very low concentrations, aqueous As(V) is reported only for the most reactive material (F168-15) at the highest initial As(III) concentration (Fig. 1D, inset).

Mass balance of arsenic species was achieved as the summation of solid-phase As(III) and As(V) concentrations and total aqueous As(III) concentration. In all samples, mass balance was within 12% of the initial As(III) concentration, suggesting that the 15 min 0.2 M oxalic acid extraction is an effective method for the desorption of arsenic species from aquifer materials. The 15 min extraction period is also acceptable considering the relatively slow transformation rates in this work. Lack of any measurable concentrations of aqueous As(V) also indicates that to correctly estimate the transformation kinetics of As(III) by natural materials, adsorbed As(V) concentration must be directly measured.

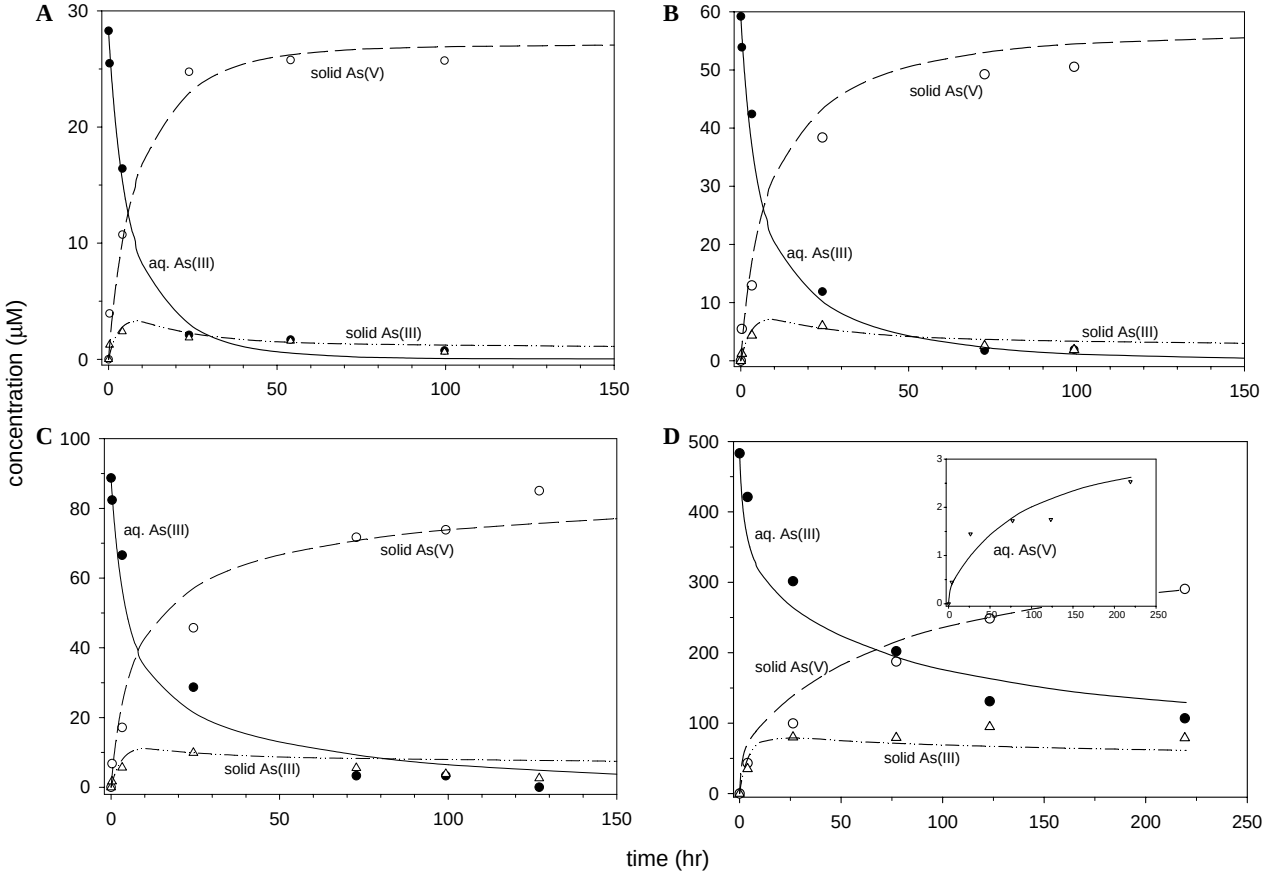

Fig. 1. Oxidation kinetics of As(III) by F168-15 material. pH 5.2, and initial [As(III)] = 28.3 μM (A), 59.2 μM (B), 88.7 μM (C), and 483.0 μM (D). All lines are model fits to the experimental data.

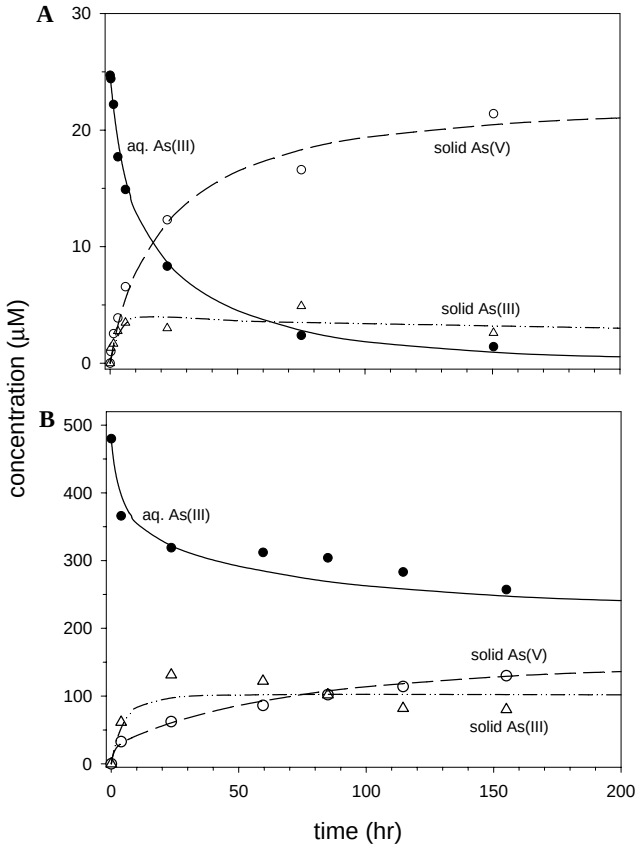

Fig. 2. Oxidation kinetics of As(III) by F168-20 material. pH 5.2, and initial [As(III)] = 24.7 μM (A), and 480.3 μM (B). All lines are model fits to the experimental data.

Arsenic displayed varying transformation rates depending on the aquifer material. The disappearance of the aqueous As(III) species and the formation of the adsorbed As(III) and As(V) species were the fastest with F168-15 material (Fig. 1), and slowest with R23AW material (Fig. 5). The extent of aqueous As(III) oxidation also follows the same order with respect to the aquifer materials. For F168-15 material, oxidation, as compared to adsorption, was clearly the dominant mechanism for aqueous As(III) removal, where more than 90% of the added As(III) at concentrations below 100 μM oxidized to As(V) (Figs. 1A–C). Oxidation was also the dominant mechanism for As(III) removal for F168-20 material at the concentration range studied here (Fig. 2). For F168-25 (Fig. 3) and F415-19 (Fig. 4) materials, however, oxidation was the dominant mechanism for As(III) removal at initial As(III) concentrations below 30 μM, whereas, oxidation and adsorption contributed nearly equally to the aqueous As(III) removal kinetics at initial As(III) concentrations near 90 μM. At initial As(III) concentrations as high as 500 μM, As(III) adsorption was clearly the dominant mechanism for the removal of aqueous As(III) for these aquifer materials (Figs. 3C and 4C). For R23AW material, As(III) adsorption was the dominant mechanism for As(III) removal at all concentrations studied here (Fig. 5).

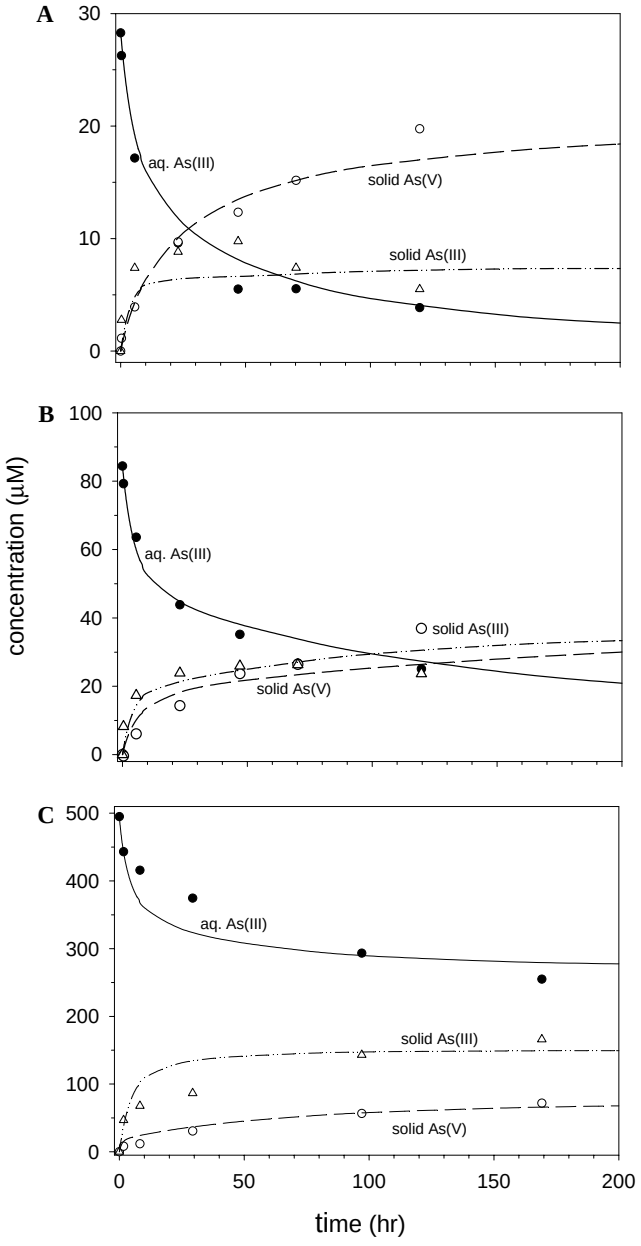

Fig. 3. Oxidation kinetics of As(III) by F168-25 material. pH 5.2, and initial [As(III)] = 28.3 μM (A), and 84.4 μM (B), and 495.4 μM (C). All lines are model fits to the experimental data.

3.2. Anaerobic and sterile controls

Arsenic(III) oxidation experiments were conducted both in the presence and absence of dissolved oxygen at pH 5.2 with F168-20 material. The same material was also used to conduct As(III) oxidation experiments in the presence of 0.1 M formaldehyde, a bactericide. In both cases, no differences in the aqueous As(III) removal and As(V) production rates were observed (results not shown here). Addition of nitrate to the same aquifer material to promote the autotrophic oxidation of As(III) by microorganisms (Oremland and Stolz, 2003) also did not result in the enhanced oxidation of As(III) (S. Hoeft, USGS, personal communica-

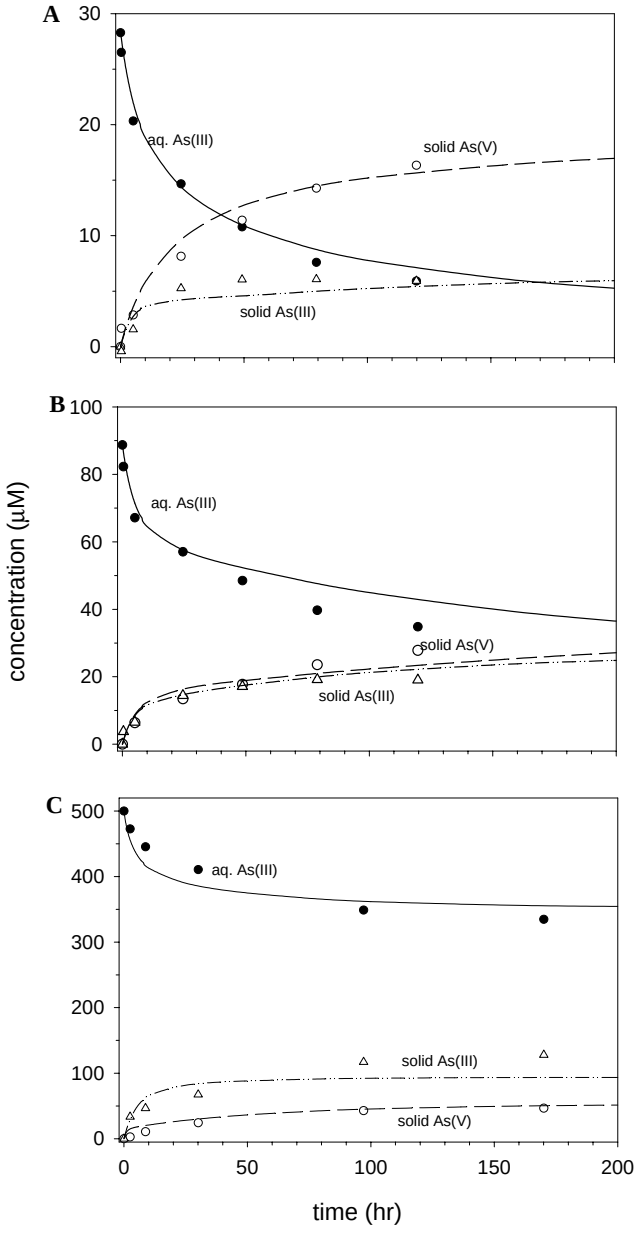

Fig. 4. Oxidation kinetics of As(III) by F415-19 material. pH 5.2, and initial [As(III)] = 28.3 μM (A), and 88.7 μM (B), and 499.8 μM (C). All lines are model fits to the experimental data.

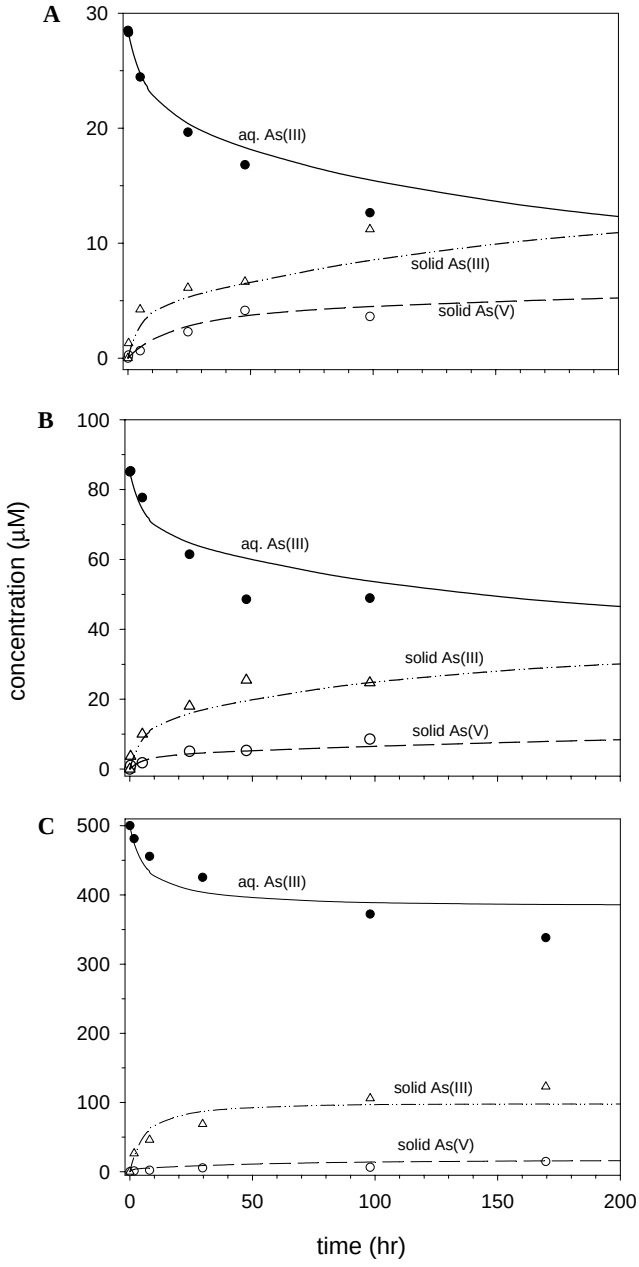

Fig. 5. Oxidation kinetics of As(III) by R23AW material. pH 5.2, and initial [As(III)] = 28.5 μM (A), and 85.1 μM (B), and 500.3 μM (C). All lines are model fits to the experimental data.

tions). These observations suggest that neither dissolved oxygen nor bacteria were responsible for As(III) oxidation.

3.3. Aquifer material properties

Previous studies cited above have shown that the extent and kinetics of As(III) oxidation may be attributed to the oxidized solid-phase manganese content of the material. Adsorption of As(III), however, is largely controlled by the oxidized iron content of the mineral (Deschamps et al., 2003). Oxidation of As(III) by Fe(III) hydroxide in lake sediment has been reported previously (De Vitre et al., 1991), possibly because of the high Fe(III):As(III) ratio. However, it is generally assumed that Fe(III) in soils with a lower Fe(III) content than lake sediments does not oxidize As(III) significantly (Oscarson et al., 1981b). The specific surface areas, and the reductively extractable iron and manganese contents of the aquifer materials used in this study are reported in Table 1. These materials possessed relatively similar specific surface areas ($0.600 \pm 0.156\ m^2\ g^{-1}$), and reductively extractable iron contents ($22.16 \pm 3.10\ \mu mol\ m^{-2}$). However, the reductively extractable manganese contents varied by a factor of six, ranging from $0.59\ \mu mol\ m^{-2}$ for R23AW material to $3.36\ \mu mol\ m^{-2}$ for F168-15 material (Table 1).

3.4. Dissolved Mn(II)

The process of oxidation of As(III) by manganese oxides leads to the production of Mn(II) (Moore et al., 1990; Scott and Morgan, 1995; Manning et al., 2002; Tournassat et al., 2002). However, dissolved manganese concentrations were less than 0.1 μM (limit of quantification) in all experiments. Experimental studies with synthetic Mn(IV) oxides have shown that dissolved manganese concentrations remained very low at pH values above approximately 5.8 (Scott and Morgan, 1995). Significant concentrations of dissolved manganese in oxic groundwater from the Cape Cod site have only been observed in samples with pH values below approximately 5.0 (Savoie and LeBlanc, 1998). These results suggest that Mn(II) binding to manganese oxide and other constituents of the solid material is sufficiently extensive to maintain very low dissolved manganese concentrations over the pH range examined in this study.

3.5. Conceptual model for arsenic–surface interactions

Similar to the previous observations regarding the kinetics of As(III) removal by oxidized manganese minerals (Scott and Morgan, 1995; Chui and Hering, 2000), the kinetics of aqueous As(III) removal by the aquifer materials used here (Figs. 1–5) do not show a simple first-order behavior. Conceptually, this suggests that As(III) removal and oxidation by aquifer material may be understood as a multi-step surface process involving (1) transport of As(III) to the surface, (2) As(III) adsorption onto the surface sites, (3) oxidation of As(III) to As(V) at the surface, (4) release of produced As(V) from the surface, and (5) As(V) adsorption to other surface sites following its production and release into solution. Adsorption of As(III) involves the displacement of surface-bound OH^- and H_2O species via a ligand exchange mechanism, whereby the As(III) anion forms an inner-sphere complex at the mineral surface (Manning et al., 1998; Nesbitt et al., 1998; Arai et al., 2001).

The As(III) adsorption process may further be characterized by the surface coordination of this species with the purely adsorptive sites where no As(III) oxidation takes place, and with the oxidative sites where As(III) is oxidized to As(V). The kinetic data suggest that within the time frame of this study, As(III) adsorption is a relatively slow process with As(III) disappearance from solution having a half-life in the order of several hours to several days depending on the aquifer material (Figs. 1–5). Previous studies of oxyanion adsorption on Cape Cod materials have found that approximately 3 days is required to reach equilibrium (Stollenwerk, 1995). Thus, on the timescale of these experiments, the rate of change of dissolved and adsorbed As(III) must be taken into consideration. The precise nature of surface complex formation of As(III) with the aquifer material surface sites is unknown, and, therefore, adsorption of As(III) on non-oxidative sites is described using a generic site, here abbreviated as $\geq$SOH,

$$\geq \mathrm{SOH} + \mathrm{H_3AsO_3} \overset{k_{f,ad}/k_{r,ad}}{\leftrightarrow} \geq \mathrm{SOAsO_2H_2} + \mathrm{H_2O} \quad (1)$$

where $k_{f,ad}$ and $k_{r,ad}$ are the forward and reverse rate constants for As(III) interaction with the adsorptive sites, respectively. It is assumed that As(III) oxidation does not take place at the surface of the adsorptive sites.

The processes involving the interaction between arsenic species and the surface manganese oxides are shown generically in Fig. 6. To obtain mass and charge balance, the reactions are shown in two dimensions. Assuming that Mn(IV) oxide is the primary oxidative site on the surface of the aquifer material, the reaction scheme in Fig. 6 depicts the formation of a As(III) precursor surface complex with forward and reverse adsorption rate constants $k_{f1,ox}$ and $k_{r1,ox}$, followed by electron transfer from the surface-bound As(III) to the Mn(IV) center with a rate constant of $k_{2,ox}$, and the release of As(V) into solution with a rate constant of $k_{3,ox}$.

Our model does not consider the regeneration of the oxidative surface sites. This assumption is reasonable for this system considering that the produced As(V) concentrations reach nearly steady-state values (Figs. 1–5), whereas significant regeneration of the surface oxidative sites would bring about a continual increase in the produced As(V) concentration. One explanation for the lack of regeneration of the surface oxidative sites could be due to the association of the produced Mn(II) with the surface Mn(IV) oxide, which would mask the surface sites from further reaction. Scott and Morgan (1995) have indeed shown that the produced Mn(II) remains associated with the surface of birnessite to a significant extent, especially at pH values above 4. Some As(V) may also remain on the manganese oxide surface following its production, as suggested by spectroscopic studies (Manning et al., 2002; Deschamps et al., 2003; Foster et al., 2003), inhibiting further As(III) interaction with that oxidative site. Another explanation

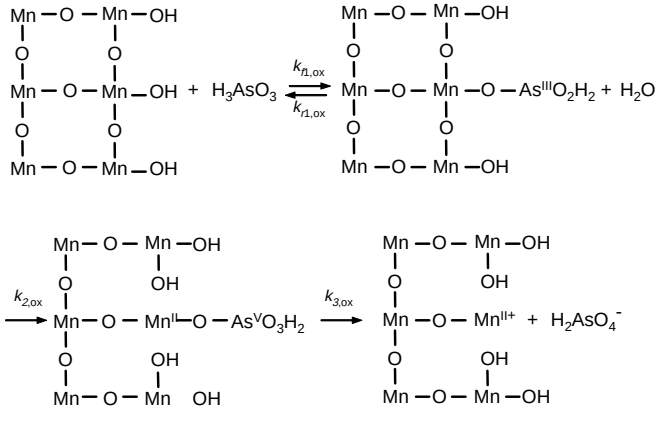

Fig. 6. Schematic showing the reversible adsorption of As(III) onto the oxidative surface Mn(IV) sites, followed by electron transfer and As(V) release. $k_{f1,ox}$ and $k_{r1,ox}$ are the forward and backward rate constants for the adsorption and desorption of As(III), respectively, $k_{2,ox}$ is the rate constant for the electron transfer reaction, and $k_{3,ox}$ is the rate constant for detachment of As(V).

may be the lack of reactivity of the newly exposed Mn(IV) metal center at the solid–solution interface.

Surface spectroscopic and proton balance studies suggest that As(III) oxidation by synthetic birnessite proceeds via a two-step process involving formation of Mn(III) as the intermediate, followed by further reduction of Mn(III) to Mn(II) at pH 4 (Nesbitt et al., 1998; Tournassat et al., 2002). We have not included the two-step oxidation process involving production of the intermediate Mn(III) in the proposed model, since the reaction stoichiometry with respect to As(III) and surface Mn(IV) species remains the same for the two models.

It is assumed that in the multi-step reaction of As(III) with MnO_2, the electron transfer and As(V) release processes are considerably faster than As(III) adsorption (Tournassat et al., 2002); i.e., the As(III) precursor surface complex is very reactive. This assumption may be justified based on the observation that As(V) interaction with natural surfaces is controlled by its adsorption to Fe(III) hydroxides compared to Mn(IV) oxides (Deschamps et al., 2003). The presence of negligible concentrations of the produced aqueous As(V) species in this study, therefore, suggests that following its production, this species interacts with the aquifer material extensively and rapidly. As discussed in the following section, under the experimental conditions of this study, this interaction may be represented as an equilibrium relationship with K_{ad} as the equilibrium constant,

$$\gtrdot\mathrm{SOH} + \mathrm{H_2AsO_4^-} \Longleftrightarrow \gtrdot\mathrm{SOAsO_3H^-} + \mathrm{H_2O}; \quad \mathrm{K_{ad}} \qquad (2)$$

3.6. Development of a macroscopic rate law for As(III) oxidation

A rigorous treatment of the reactive functional groups of natural surfaces with mixtures of mineral phases and their electrical double layer properties is a complicated task. Part of this difficulty arises from the uncertainties in the estimation of the surface densities of reference mineral phases and the associated surface coatings that are available for reaction with the solution phase species (Davis et al., 2004). Here, we have used the Generalized Composite (GC) approach where solute–surface interactions are described by mass balance and reaction thermodynamic expressions containing "generic" surface functional groups. The relevant stoichiometry and equilibrium constants for these expressions are estimated by fitting experimental data for the entire mineral assemblage (Davis et al., 1998; Westall et al., 1998). Even though the GC approach is generally developed for equilibrium solute adsorption, we have used it to develop a set of mass action equations to model the kinetics of arsenic interaction and redox transformation at the surface of aquifer materials. The GC approach also neglects any surface electrostatic correction factors, and as such, requires fewer fitting parameters, and is computationally efficient when incorporated in reactive solute transport models. The general goal of this approach is to develop the simplest possible model with the least number of fitting parameters that describes the main characteristics of solute–surface interaction in a chemically heterogeneous system (Davis et al., 1998).

The reactions depicted in Eqs. (1) and (2), and in Fig. 6 were used to model the experimental data, with the corresponding equilibrium and rate constants as the fitting parameters. To reduce the number of fitting parameters, certain simplifying assumptions were made in the treatment of the kinetic data. For chemical reactions in series, such as the ones depicted in Fig. 6, when the intermediate complexes (i.e., adsorbed As(III) and As(V) complexes at the oxidative sites) are so reactive that they do not accumulate at an appreciable level compared to the reactants and the products, steady-state condition with respect to these species may be assumed (Espenson, 1995). The adsorbed As(III) and As(V) concentrations at the surface of the oxidative sites cannot be directly measured in this system. However, based on the results of several previous studies of As(III) oxidation by synthetic MnO_2 minerals, we have assumed that the concentration of As(III) precursor surface complex, ($\gtrdot\mathrm{MnOAs^{(III)}O_2H_2}$; Fig. 6) is relatively small at any given time, and as such, reaches a steady-state value. Setting the formation rate of the As(III) precursor surface complex equal to zero (i.e., $\frac{\mathrm{d}[\gtrdot\mathrm{MnOAs^{(III)}O_2H_2}]}{\mathrm{d}t} = 0$), and solving for the steady-state concentration of $\gtrdot\mathrm{MnOAs^{(III)}O_2H_2}$ species from the set of reactions in Fig. 6, the formation rate of the aqueous As(V) species may be obtained as,

$$\frac{\mathrm{d}[\mathrm{H_2AsO_4^-}]}{\mathrm{d}t} = k'_{\mathrm{ox}}[\gtrdot\mathrm{MnOH}][\mathrm{H_3AsO_3}], \qquad (3)$$

where, the apparent rate constant $k'_{\mathrm{ox}} = \frac{k_{\mathrm{f1,ox}}k_{3,\mathrm{ox}}}{k_{\mathrm{r1,ox}}+k_{3,\mathrm{ox}}}$ if $k_{2,\mathrm{ox}} \gg k_{3,\mathrm{ox}}$, and $k'_{\mathrm{ox}} = \frac{k_{\mathrm{f1,ox}}k_{2,\mathrm{ox}}}{k_{\mathrm{r1,ox}}+k_{2,\mathrm{ox}}}$ if $k_{3,\mathrm{ox}} \gg k_{2,\mathrm{ox}}$. The steady-state assumption also implies that $k_{\mathrm{r1,ox}} + k_{2,\mathrm{ox}}$ (or $k_{3,\mathrm{ox}}$) $\gg k_{\mathrm{f1,ox}}$, which suggests a slow rate of As(III) adsorption onto the oxidative sites compared to the As(III) transformation and As(V) release rates. The steady-state assumption simplifies the kinetic formulation considerably by combining four rate constants (Fig. 6) into one, k'_{ox}.

Obtaining a quantitative fit of experimental adsorption data over a wide range of chemical conditions on Cape Cod aquifer materials with semi-empirical surface complexation models required considering strong and weak binding sites (Davis et al., 1998). This likely reflects the variation in the adsorption site energies on complex mineral surfaces. For the As(III) concentration range used here, best fits to the data were obtained by considering two sites with differing interaction energies for both the purely adsorptive sites and the oxidative sites. Since this study involves adsorption and oxidation kinetics of arsenic species in the presence of a solid surface, these sites are termed fast and slow, in analogy to the strong and weak sites used for adsorption equilibrium. We have further assumed a constant total surface density for the adsorptive sites at 2.31 sites $\mathrm{nm^{-2}}$ (equivalent to 3.84 μmol $\mathrm{m^{-2}}$) for all aquifer materials as proposed by Davis and Kent (1990). This

Table 2
Equilibrium and kinetic expressions and constants used to model the data [a]

Reaction[b]	k or $\log K$[b,c]	Ref.
$H_3AsO_3 \iff H^+ + H_2AsO_3^-$	−9.15	1
$H_3AsO_4 \iff H^+ + H_2AsO_4^-$	−2.3	1
$H_3AsO_4 \iff 2H^+ + HAsO_4^{2-}$	−9.46	1
$H_3AsO_4 \iff 3H^+ + AsO_4^{3-}$	−21.11	1
$\geq S^fOH + H_3AsO_3 \leftrightarrow \geq S^fOAsO_2H + H_2O$	$k^f_{f,ad} = 2.43 \times 10^{-2}$ M^{-1} s^{-1} $k^f_{r,ad} = 5.25 \times 10^{-7}$ s^{-1}	2
$\geq S^sOH + H_3AsO_3 \leftrightarrow \geq S^sOAsO_2H + H_2O$	$k^s_{f,ad} = 6.85 \times 10^{-3}$ M^{-1} s^{-1} $k^s_{r,ad} = 4.72 \times 10^{-5}$ s^{-1}	2
$\geq Mn^fOH + H_3AsO_3 \rightarrow H_3AsO_4 +$ other products[d]	$k^f_{ox} = 6.28 \times 10^{-1}$ M^{-1} s^{-1}	2
$\geq Mn^sOH + H_3AsO_3 \rightarrow H_3AsO_4 +$ other products[d]	$k^s_{ox} = 1.25 \times 10^{-2}$ M^{-1} s^{-1}	2
$\geq S^fOH + H_2AsO_4^- \iff \geq S^fOAsO_3H^- + H_2O$	6.37	2
$\geq S^sOH + H_2AsO_4^- \iff \geq S^sOAsO_3H^- + H_2O$	5.06	2
$\geq MnOH \iff \geq MnO^- + H^+$	−6.2 (for both oxidative sites)	2

1, Smith and Martell (1976); 2, this work.
[a] Constants for all surface reactions estimated using data for F168-15 material.
[b] "f" and "s" in the superscripts refer to fast and slow sites, respectively, and "f" and "r" in the subscripts refer to forward and reverse rate constants, respectively.
[c] Constants given for $I = 0$.
[d] See Fig. 6 and the text for the explanation of these reactions.

choice is in keeping with the development of a self-consistent thermodynamic database that may be applied to model solute adsorption onto natural composite mineral surfaces.

Table 2 shows the set of reactions used to describe the kinetics of arsenic interaction with the aquifer material. These reactions involve five rate and equilibrium constants for each fast and slow site that need to be optimized to model the data. Kinetic data from the most reactive material (F168-15) were fitted with the constants in Table 2, as well as with the total surface density for both fast and slow oxidative sites. The F168-15 material possessed the highest reductively extractable manganese content (Table 1), and the fastest As(III) removal and As(V) production rates of all materials (Fig. 1). The constants obtained were then used to simulate As(III) oxidation kinetics by other aquifer materials. In this case, however, since each material had a different reactivity with respect to As(III) oxidation, and a different reductively extractable manganese content (Table 1), the oxidative site densities were used as the only fitting parameters for individual materials; i.e., the rate and equilibrium constants were the same for all materials, and as described above, the total density of adsorptive sites were estimated from the specific surface area measurements. The approach used here, where the parameters were estimated based on only one material and used for materials not used originally in the model development, is intended to validate the proposed model for different conditions.

The reaction parameters were determined by fitting the model to the observed aqueous As(III), and adsorbed As(III) and As(V) data for F168-15 material that was reacted with initial As(III) concentrations that ranged from 30 to 500 μM (Fig. 1). Initial parameter values were estimated from observations at both 30 and 500 μM, and then all of the reaction parameters were estimated simultaneously using the four different initial As(III) concentrations by UCODE. The values of the calibrated equilibrium and rate constants for the F168-15 material are reported in Table 2 and the fitted site densities for the oxidative sites are reported in Table 3. For the non-oxidative site densities, the best fit to the ktinetic data

Table 3
Fitted densities for the oxidative sites

Aquifer material	$\geq Mn^fOH$ (μmol m^{-2})	$\geq Mn^sOH$ (μmol m^{-2})
F168-15	0.129	0.665
F168-20	0.053	0.303
F168-25	0.032	0.106
F415-19	0.049	0.134
R23AW	0.013	0.046

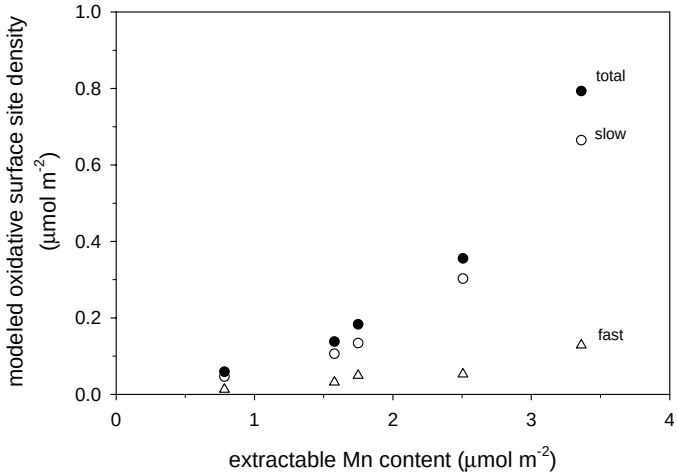

Fig. 7. Reductively extractable manganese content vs. the modeled oxidative surface site density. (●) Total density of the fitted sites, (○) fitted density of the slow sites, and (△) fitted density of the fast sites.

for F168-15 material was provided by a fast:slow site ratio = 0.045. For other aquifer materials, the equilibrium and rate constants were fixed, the non-oxidative site densities were calculated from the measured surface area (Davis and Kent, 1990) using a fast:slow site ratio = 0.045, and the total surface density for both fast and slow oxidative sites were obtained by fitting the data for individual materials (Table 3).

Fig. 7 shows the comparison between the reductively extractable Mn(IV) content and the modeled oxidative surface site density for the five aquifer materials. Even though there is a positive correlation between the two parameters, this correlation is non-linear. The ratio of the modeled site density to the extractable manganese varies from approximately 5% for the least reactive material to 24% for the most reactive material. One explanation for the lack of a linear relationship between the measured and modeled oxidative site densities may be that differences in the properties of manganese oxides in the aquifer materials may reflect differences in weathering processes from which they are formed. This could be especially plausible in the case of F168 samples that were collected from the same core at depths of 15–20 ft. (F168-15), 20–25 ft. (F168-20), and 25–30 ft. (F168-25). The reductively extracted manganese content decreases with the depth in this core (Table 1). This observation is consistent with a conceptual model for oxidation of glacial outwash sediments whereby the extent of sediment oxidation increases with decreasing depth (Böhlke et al., 2002). Alternatively, it could be a result of more extensive weathering at shallower depths driven by lower pH values (Kent et al., 1995), heterogeneities in the distribution of minerals whose weathering results in the formation of manganese oxide minerals, or a remnant of past groundwater-chemical conditions that have since been flushed from the system.

The modeled fast and slow oxidative site densities are also shown in Fig. 7. The fast:slow ratios for these sites varied between 17 and 37% among the different aquifer materials. It is possible that the heterogeneous nature of the oxidative sites within the aquifer materials in this study is due to the presence of manganese oxides with variable composition and/or levels of crystallinity. The presence of Mn(IV) oxides with various degrees of crystallinity has been suggested previously (Tournassat et al., 2002). The variations in the degree of crystallinity of birnessite may be inferred from the observed variations in the initial oxidation rates of As(III) among several studies (Oscarson et al., 1983; Scott and Morgan, 1995; Tournassat et al., 2002). Alternatively, fast oxidative sites might represent sites at or near the surface. Once these sites have reacted, further oxidation requires that As(III) overcome the diffusion resistance required to reach internal oxidative sites. This explanation is in analogy to the diffusion-controlled adsorption of As(V) onto hydrous ferric oxide as proposed by Fuller et al. (1993), where sites closer to the surface of aggregates were assumed to reach equilibrium faster than the internal sites.

3.7. pH dependence

The effect of pH on As(III) removal rate by F168-15 material was studied over a pH range of 4.1 to 6.9 (Fig. 8). The As(III) removal rate as well as the As(V) production rate decreased with a pH increase. This decrease, however, is relatively small, with an almost doubling of aqueous As(III) half-life as pH increases from 4.1 to 6.9 (Fig. 8). The pH dependence of As(III) interaction with synthetic birnessite and manganite was suggested to be due to the slower adsorption of As(III) onto these minerals as the pH increases (Scott and Morgan, 1995; Chui and Hering, 2000). It was proposed that this behavior may be explained by the acid–base character of the ≥MnOH sur-

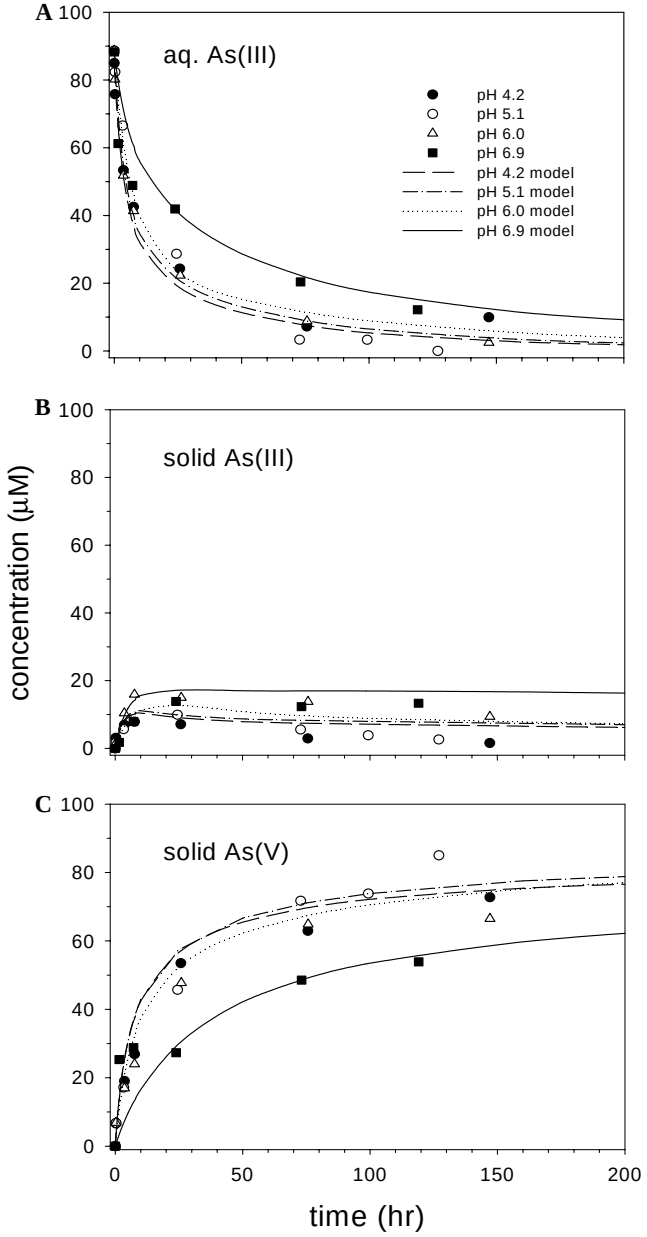

Fig. 8. pH dependence of As(III) oxidation kinetics for F168-15 material.

face groups, where a pH increase would increase $\geq MnO^-$ concentration at the expense of $\geq MnOH$ concentration.

In this work, the trend in oxidation with increasing pH can be incorporated into the model by simply considering a pK_a of 6.2 for the acid–base reaction of the oxidative surface sites (Table 2). Given that the concentration of H_3AsO_3 species does not change within the pH range studied here (Table 2), the decrease in concentration of the oxidative $\geq MnOH$ sites with increase in pH would cause a decrease in the formation rate of As(V) species (Fig. 8C), according to Eq. (3). A higher adsorbed As(III) concentration at a higher pH (Fig. 8B) then is due to the diminished competition between the oxidative and adsorptive sites for As(III) caused by the enhanced deprotonation of the oxidative sites at a higher pH.

Scott and Morgan (1995) have reported a pK_a of 4.9 for the deprotonation of the surface $\geq MnOH$ for synthetic birnessite, as obtained by acid–base titrations in the presence of 0.1 M $NaClO_4$. Other than structural differences between natural and synthetic manganese oxides affecting their surface charge characteristics, and the fact that different species of manganese oxides may exist in a given natural sample, the relatively high pK_a of 6.2 reported in this study may be also due to the presence of adsorbed cations on natural as opposed to synthetic manganese oxides. Cations were continually released form the hydrated aquifer material in this system, as evidenced by a gradual increase in pH in an unbuffered suspension of this material. Cation adsorption increases with pH, leading to an increase in the point of zero charge of the surface, which in turn leads to a higher apparent surface pK_a.

3.8. Effect of phosphate

Fig. 9 shows the effect of 1 mM phosphate on the kinetics of arsenic interaction with F168-15 material. For comparison purposes, the data for arsenic interaction with the aquifer material in the absence of phosphate are shown. Phosphate somewhat diminishes the rate of As(III) removal (Fig. 9A) as well as the rate of As(V) production (Fig. 9C), even though at longer times in both systems, aqueous As(III) is removed and As(V) is produced at nearly equal concentrations. However, the effect of phosphate on the kinetics of As(III) adsorption onto the non-oxidative sites is nearly negligible (Fig. 9B). The concentration of aqueous As(V) was below the detection limit in the presence of phosphate, indicating that phosphate did not result in the release of adsorbed As(V) through competition for the surface adsorption sites. In a recent field injection study at the USGS groundwater research site at Cape Cod, MA, Kent and Fox (2004) observed that a phosphate concentration of 620 μM could mobilize As(V) at concentrations as high as 0.07 μM. The latter concentration is far lower than arsenic concentrations studied and detected here. It may be that in this system, phosphate addition resulted in the release of small arsenic concentrations that were below the detection limit. It is also expected that large enough concentrations of phosphate or other anions, such as natural organic matter, silicic acid, or bicarbonate could influence As(III) and As(V) partition reactions (Wilkie and Hering, 1996; Swedlund and Webster, 1999; Meng et al., 2000; Appelo et al., 2002; Waltham and Eick, 2002).

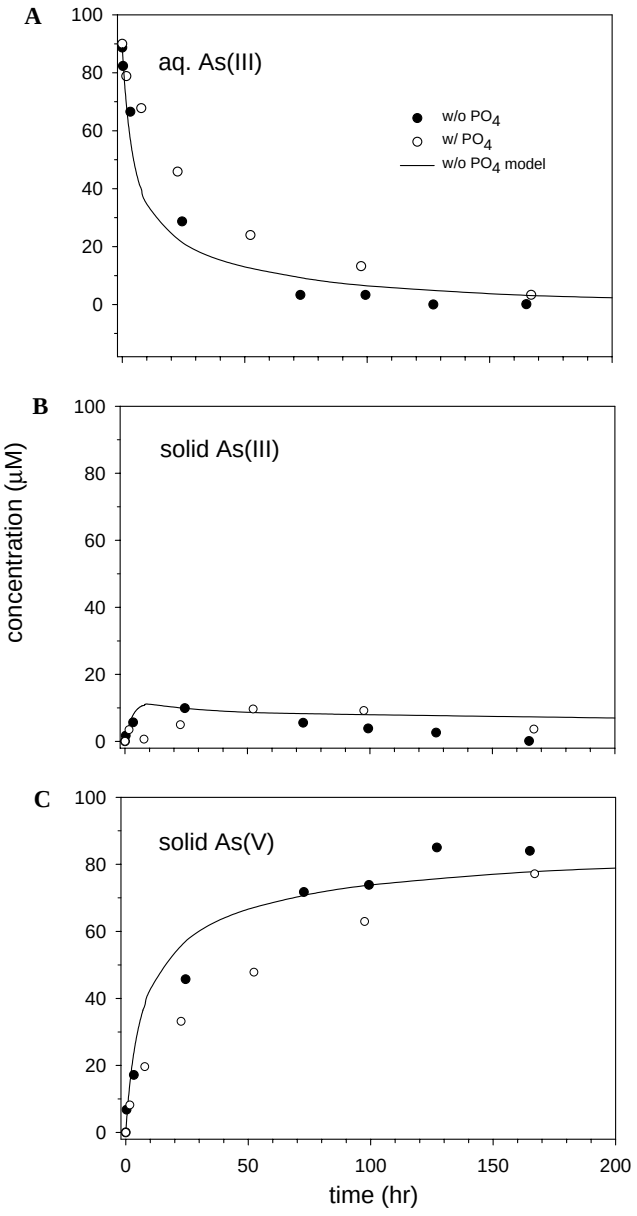

Fig. 9. Effect of 1 mM Na_2HPO_4 on As(III) oxidation kinetics by F168-15 material. pH 5.2, and initial [As(III)] = 90.0 and 88.7 μM in the presence and absence of phosphate, respectively.

The total estimated concentrations of the oxidative and adsorptive surface sites for F168-15 material were approximately 280 and 1630 μM, respectively, in the batch systems. Almost all phosphate was removed from solution within the first 7 h of the experiment (data not shown here). Given that the concentration of the adsorptive surface sites was far in excess of the initial As(III) and phosphate concentrations, it is not surprising that phosphate did not influence the adsorption kinetics of As(III) and As(V) onto

these sites. Our observations regarding the slightly slower kinetics of the aqueous As(III) removal and As(V) production in the presence of phosphate, therefore, suggest phosphate interaction with oxidative sites.

4. Conclusions and implications

The results of this study suggest that oxidation of As(III) by aquifer materials might make natural attenuation of arsenic viable. The dominance of oxidation vs. adsorption mechanisms for the removal of As(III) at timescales studied here depends on the concentration of As(III), as well as the Mn:Fe ratio of the aquifer material. The experimental and modeling results in this study show that for reductively extractable Mn:Fe ratios greater than 0.1, As(III) oxidation would be the dominant pathway, and at ratios less than 0.02, As(III) adsorption would be the dominant pathway for the removal of arsenic from solution. Therefore, the removal of As(III) from solution along the flow paths may not be necessarily all due to its oxidation under relatively short timescales. However, under field-relevant timescales, even for aquifer materials with a very high iron content, the reversibility of As(III) adsorption to the purely adsorptive sites would bring about its eventual interaction with and oxidation by the oxidative sites.

Studies involving As(III) oxidation by synthetic MnO_2 show that As(III) removal rates span over an order of magnitude for similar molar As:Mn ratios (Oscarson et al., 1983; Moore et al., 1990; Scott and Morgan, 1995; Tournassat et al., 2002). The As(III) removal rates obtained in this study are closest to the rate reported by Tournassat et al. (2002), who observed by far the slowest As(III) removal rate of all previous studies with a half-life of 35 h for a molar As:Mn ratio of 0.44 at pH 5.0. For the most reactive material in this study (F168-15), we observed a half-life of 35 h for a molar As:Mn ratio of 0.35 at pH 5.2 (Fig. 1D). Tournassat et al. (2002) attributed their very low observed As(III) removal rate to the highly crystalline nature of their birnessite sample. The correspondence between the rates in the two studies may suggest that the manganese oxide in the aquifer material is perhaps also highly crystalline.

Results of a field-scale transport experiment verify the importance of As(III) adsorption and oxidation by aquifer materials (Stadler et al., 2001). Arsenic(III) was injected into oxic, mildly acidic (pH 5.7), low ionic-strength groundwater adjacent to the site where the R23AW material was obtained. Aqueous samples collected 2.2 m downgradient from the injection showed a significant delay in As(III) breakthrough relative to that of the chemically inert Br^- tracer, and that, in contrast to Br^- concentrations, peak As(III) concentrations were much lower than the injected concentrations. As(V) concentrations were considerably lower than As(III) concentrations during breakthrough. A quantitative estimate of the As(III) oxidation rate cannot be made in the absence of accurate accounting for adsorption of As(III) and As(V). However, the results underscore the relevance of adsorption and oxidation on arsenic transport, as indicated by our experimental results.

The likely role of manganese oxides in As(III) oxidation suggested by the results of this study lends support to the link between development of oxidizing conditions and fate and transport of arsenic in aquifers. Development of oxidizing conditions in glacial outwash materials is influenced by the time required to oxidize pyrite, other sulfide minerals, and Fe(II) associated with primary minerals in the solid material (Böhlke et al., 2002). The absence of any significant decreases in dissolved oxygen concentrations after 25 years of transport in western Cape Cod illustrates the extent to which these materials have been oxidized (Böhlke et al., 1999). Complete oxidation of Fe(II) minerals is probably not required because the development of Fe(III) hydroxide coatings eventually insulates Fe(II) in the interior of mineral grains from dissolved oxygen and other oxidants in groundwater (White and Peterson, 1996). Indeed, the persistence of sulfide minerals in aquifer materials from the site is indicated by the results of chemical extractions, which suggest that 50–75% of the total arsenic is associated with sulfide minerals (Kent and Fox, 2004). Thus, oxidative weathering reactions can play a central role in the fate of naturally occurring arsenic. Oxidation of pyrite and other sulfide minerals releases arsenic (Böhlke, 2002). Oxidation of Fe(II)-containing minerals results in the formation of secondary Fe(III) hydroxides in coatings on mineral grains (Coston et al., 1995; Penn et al., 2001), which have a high affinity for adsorption of inorganic arsenic species (e.g., Appelo et al., 2002; Kneebone et al., 2002; Dixit and Hering, 2003; Stollenwerk, 2003). Manganese oxide minerals formed during oxidative mineral weathering reactions provide a strong oxidant for As(III) to As(V). Adsorbed As(V) is subject to release in response to changing groundwater chemical conditions, such as pH and concentrations of phosphate and other competing ions (Belzile and Tessier, 1990; Kent and Fox, 2004).

Acknowledgments

A.A. is grateful to the University of Maine for granting him sabbatical leave in 2004. Patricia Fox and Matthias Kohler are acknowledged for sharing their valuable ideas. Michael Borda, Suvasis Dixit, Andrea Foster, and two anonymous reviewers are acknowledged for their constructive comments on the manuscript. Partial funding was provided by the USGS Water Resources Division National Research Program, and Toxic Substances Hydrology Program.

Associate editor: Donald L. Sparks

References

Ahmann, D., Krumholz, H.F., Hemond, H.F., Lovley, D.R., Morel, F.M.M., 1997. Microbial mobilization of arsenic from sediments of the Aberjona watershed. *Environ. Sci. Technol.* **31**, 2923–2930.

Appelo, C.A.J., van der Weiden, M.J.J., Tournassat, C., Charlet, L., 2002. Surface complexation of ferrous iron and carbonate on ferrihydrite and the mobilization of arsenic. *Environ. Sci. Technol.* **36**, 3096–3103.

Arai, Y., Elzinga, E.J., Sparks, D.L., 2001. X-ray absorption spectroscopic investigation of arsenite and arsenate adsorption at the aluminum oxide–water interface. *J. Colloid Interface Sci.* **235**, 80–88.

Arai, Y., Sparks, D.L., Davis, J.A., 2005. Arsenate adsorption mechanisms at the allophane–water interface. *Environ. Sci. Technol.* **39**, 2537–2544.

Barber, L.B., 1990. Geochemical heterogeneity in a glacial outwash aquifer: effect of particle size and mineralogy on sorption of nonionic organic solutes. Ph.D. thesis, Univ. Colorado.

Banfield, J.F., Hamers, R.J., 1997. Processes at minerals and surfaces with relevance to microorganisms and prebiotic synthesis. In: Banfield, J.F., Nealson, K.H. (Eds.), *Reviews in Mineralogy, Advances in Mineralogy*, vol. 35. Mineralogical Society of America, pp. 81–122.

Bau, M., Alexander, B., Chesley, J.T., Dulski, P., Brantley, S.L., 2004. Mineral dissolution in the Cape Cod Aquifer, Massachusetts, USA: 1. Reaction stoichiometry and impact of accessory feldspar and glauconite on strontium isotopes, solute concentrations, and REY distribution. *Geochim. Cosmochim. Acta* **68**, 1199–1216.

Bednar, A.J., Garbarino, J.R., Ranville, J.F., Wildeman, T.R., 2002. Preserving the distribution of inorganic arsenic species in groundwater and acid mine drainage samples. *Environ. Sci. Technol.* **36**, 2213–2218.

Belzile, N., Tessier, A., 1990. Interactions between arsenic and iron oxyhydroxides in lacustrine sediments. *Geochim. Cosmochim. Acta* **54**, 103–109.

Böhlke, J.K., 2002. Groundwater recharge and agricultural contamination. *Hydrogeol. J.* **10**, 153–179.

Böhlke, J.K., Smith, R.L., Coplen, T.B., Busenberg, E., LeBlanc, D.R., 1999. Recharge conditions and flow velocities of contaminated and uncontaminated ground waters at Cape Cod, Massachusetts: evaluation of δ-^{2}H, δ-^{18}O, an dissolved gases. In: Marganwalp, D.W., Buxton, H.T. (Eds.), *Water Resour. Invest. Rept. 99-4018C*. US Geological Survey, pp. 337–348.

Böhlke, J.K., Wanty, R., Tuttle, M., Delin, G., Landon, M., 2002. Denitrification in the recharge area and discharge area of a transient agricultural nitrate plume in a glacial outwash sand aquifer, Minnesota. *Water Resour. Res.* **38**, 1105, doi:10.1029/2001WR000663.

Brannon, J.M., Patrick, W.H., 1987. Fixation, transformation, and mobilization of arsenic in sediment. *Environ. Sci. Technol.* **21**, 450–459.

Chui, V.Q., Hering, J.G., 2000. Arsenic adsorption and oxidation at manganite surface. 1. Method for simultaneous determination of adsorbed and dissolved arsenic species. *Environ. Sci. Technol.* **34**, 2029–2034.

Coston, J.A., Fuller, C.C., Davis, J.A., 1995. Pb^{2+} and Zn^{2+} adsorption by a natural aluminum- and iron-bearing surface coating on an aquifer sand. *Geochim. Cosmochim. Acta* **59**, 3535–3547.

Cummings, D.E., Caccavo Jr., F., Fendorf, S., Rosenzweig, R.F., 1999. Arsenic mobilization by the dissimilatory Fe(III)-reducing bacterium *Shewanella alga* BrY. *Environ. Sci. Technol.* **33**, 723–729.

Curtis, G.P., 2005. *Documentation and Applications of the Reactive Geochemical Transport Model RATEQ*, NUREG Report CR-6871, US Nuclear Regulatory Commission, Rockville, MD. 97 pp.

Darland, J.E., Inskeep, W.P., 1997. Effects of pH and phosphate competition on the transport of arsenate. *J. Environ. Qual.* **26**, 1133–1139.

Davis, J.A., Kent, D.B., 1990. Surface complexation modeling in aqueous geochemistry. In: *Reviews in Mineralogy, Mineral–Water Interface Geochemistry*, vol. 23, Mineralogical Society of America, pp. 177–260.

Davis, J.A., Coston, J.A., Kent, D.B., Fuller, C.C., 1998. Application of the surface complexation concept to complex mineral assemblages. *Environ. Sci. Technol.* **32**, 2820–2828.

Davis, J.A., Meece, D.E., Kohler, M., Curtis, G.P., 2004. Approaches to surface complexation modeling of uranium(VI) adsorption of aquifer sediments. *Geochim. Cosmochim. Acta* **68**, 3621–3641.

Deschamps, E., Ciminelli, V.S.T., Weidler, P.G., Ramos, A.Y., 2003. Arsenic sorption onto soils enriched in Mn and Fe minerals. *Clay Clay Miner.* **51**, 197–204.

De Vitre, R., Belzile, N., Tessier, A., 1991. Speciation and adsorption of arsenic on diagenetic iron oxyhydroxides. *Limnol. Oceanogr.* **36**, 1480–1485.

Dixit, S., Hering, J.G., 2003. Comparison of arsenic(V) and arsenic(III) sorption onto iron oxide minerals: implications for arsenic mobility. *Environ. Sci. Technol.* **37**, 4182–4189.

Dzombak, D.A., Morel, F.M., 1990. *Surface Complexation Modeling: Hydrous Ferric Oxide*. Wiley, New York, NY.

Espenson, J.H., 1995. *Chemical Kinetics and Reaction Mechanisms*, second ed. McGraw-Hill, New York.

Fendorf, S.E., Eick, M., Grossl, P., Sparks, D.L., 1997. Arsenate and chromate retention mechanisms on goethite. 1. Surface structure. *Environ. Sci. Technol.* **31**, 315–319.

Foster, A.L., Brown, G.E., Parks, G.A., 2003. X-ray absorption fine structure study of As(V) and Se(IV) sorption complexes on hydrous Mn oxides. *Geochim. Cosmochim. Acta* **67**, 1937–1953.

Fuller, C.C., Davis, J.A., Waychunas, G.A., 1993. Surface chemistry of ferrihydrite: 2. Kinetics of arsenate adsorption and coprecipitation. *Geochim. Cosmochim. Acta* **57**, 2271–2282.

Fuller, C.C., Davis, J.A., Coston, J.A., Dixon, E., 1996. Characterization of metal adsorption variability in a sand and gravel aquifer, Cape Cod, Massachusetts, USA. *J. Contam. Hydrol.* **22**, 165–187.

Gräfe, M., Nachtegaal, M., Sparks, D.L., 2004. Formation of metal-arsenate precipitates at the goethite–water interface. *Environ. Sci. Technol.* **38**, 6561–6570.

Harrington, J.M., Fendorf, S.E., Rosenzweig, R.F., 1998. Biotic generation of arsenic(III) in metal(loid)-contaminated lake sediments. *Environ. Sci. Technol.* **32**, 2425–2430.

Harvey, C.F., Swartz, C.H., Badruzzaman, A.B.M., Keon-Blute, N., Yu, W., Ali, M.A., Jay, J., Beckie, R., Niedan, V., Brabander, D., Oates, P.M., Ashfaque, K.N., Islam, S., Hemond, H.F., Ahmed, M.F., 2002. Arsenic mobility and groundwater extraction in Bangladesh. *Science* **298**, 1602–1606.

Höhn, R., Isenbeck-Schröter, M., Niedan, V., Scholz, C., Tretner, A., Jann, S., Stadler, S., Kent, D.B., Davis, J.A., Jakobsen, R., 2001. Tracer test with arsenic(V) in an iron-reducing environment at the USGS Cape Cod Site (MA, USA). In: Cidu, R. (Ed.), *Water–Rock Interaction 2000*. Balkema, Lisse, Italy, pp. 1099–1102.

Horneman, A., van Geen, A., Kent, D.V., Mathe, P.E., Zheng, Y., Dhar, R.K., O'Connell, S., Hoque, M.A., Aziz, Z., Shamsudduha, M., Seddique, A.A., Ahmed, K.M., 2004. Decoupling of As and Fe release to Bangladesh groundwater under reducing conditions, Part I.: evidence from sediment profiles. *Geochim. Cosmochim. Acta* **68**, 3459–3473.

Johnson, D.L., Pilson, M.E.Q., 1975. The oxidation of arsenite in seawater. *Environ. Lett.* **8**, 157–171.

Kent, D.B., Davis, J.A., Anderson, L.C.D., Rea, B.A., 1995. Transport of chromium and selenium in a pristine sand and gravel aquifer: role of adsorption processes. *Water Resour. Res.* **31**, 1041–1050.

Kent, D.B., Davis, J.A., Anderson, L.C.D., Rea, B.A., Waite, T.D., 1994. Transport of chromium and selenium in the suboxic zone of a shallow aquifer: influence of redox and adsorption reactions. *Water Resour. Res.* **30**, 1099–1114.

Kent, D.B., Fox, P.M., 2004. The influence of groundwater chemistry on arsenic concentrations and speciation in a quartz sand and gravel aquifer. *Geochem. Trans.* **5**, 1–12.

Kohler, M., Curtis, G.P., Kent, D.B., Davis, J.A., 1996. Experimental investigation and modeling of uranium(VI) transport under variable chemical conditions. *Water Resour. Res.* **32**, 3539–3551.

Kneebone, P.E., O'Day, P.A., Jones, N., Hering, J.G., 2002. Deposition and fate of arsenic in iron- and arsenic-enriched reservoir sediments. *Environ. Sci. Technol.* **36**, 381–386.

Kuhn, A., Sigg, L., 1993. Arsenic cycling in eutrophic Lake Greifen, Switzerland—Influence of seasonal redox processes. *Limnol. Oceanogr.* **38**, 1052–1059.

LeBlanc, D.R., 1984. Sewage plume in a sand and gravel aquifer, Cape Cod, Massachusetts, U.S. Geological Survey Water-Supply Paper 2218, 28.

LeBlanc, D.R., Garabedian, S.P., Hess, K.M., Gelhar, L.W., Quadri, R.D., Stollenwerk, K.G., Wood, W.W., 1991. Large-scale natural-gradient tracer test in sand and gravel, Cape Cod, Massachusetts: 1. Experimental design and observed tracer movement. *Water Resour. Res.* **27**, 895–910.

Manning, B.A., Goldberg, S., 1996. Modeling competitive adsorption of arsenate with phosphate and molybdate on oxide minerals. *Soil Sci. Soc. Am. J.* **60**, 121–131.

Manning, B.A., Goldberg, S., 1997. Adsorption and stability of arsenic(III) at the clay mineral–water interface. *Environ. Sci. Technol.* **31**, 2005–2011.

Manning, B.A., Fendorf, S.E., Goldberg, S., 1998. Surface structures and stability of arsenic(III) on goethite: spectroscopic evidence for inner-sphere complexes. *Environ. Sci. Technol.* **32**, 2383–2388.

Manning, B.A., Fendorf, S.E., Bostick, B., Suarez, D.L., 2002. Arsenic(III) oxidation and arsenic(V) adsorption reactions on synthetic birnessite. *Environ. Sci. Technol.* **36**, 976–981.

Manzurul Hassan, M., Atkins, P.J., Dunn, C.E., 2003. The spatial pattern of risk from arsenic poisoning: a Bangladesh case study. *J. Environ. Sci. Health* **A38**, 1–24.

Mariner, P.E., Holzmer, F.J., Jackson, R.E., Meinardus, H.W., Wolf, F.G., 1996. Effects of high pH on arsenic mobility and on aquifer permeability along the adjacent shoreline, Commencement Bay Superfund Site, Tacoma, Washington. *Environ. Sci. Technol.* **30**, 1645–1651.

McArthur, J.M., Ravenscroft, P., Safiulla, S., Thirlwall, M.F., 2001. Arsenic in groundwater: testing pollution mechanisms for sedimentary aquifers in Bangladesh. *Water Resour. Res.* **37**, 109–117.

McCreadie, H., Blowes, D.W., Ptacek, C.J., Jambor, J.L., 2000. Influence of reduction reactions and solid-phase composition on porewater concentrations of arsenic. *Environ. Sci. Technol.* **34**, 3159–3166.

Meng, X., Bang, S., Korfiatis, G.P., 2000. Effects of silicate, sulfate, and carbonate on arsenic removal by ferric chloride. *Water Resour.* **34**, 1255–1261.

Moore, J.N., Walker, J.R., Hayes, T.H., 1990. Reaction scheme for the oxidation of As(III) to As(V) by birnessite. *Clay Clay Miner.* **38**, 549–555.

National Research Council, 1999. Arsenic in Drinking Water. National Academy Press, Washington, DC.

Nesbitt, H.W., Canning, G.W., Bancroft, G.M., 1998. XPS study of reductive dissolution of 7 Å-birnessite by H_3AsO_3, with constraints on reaction mechanism. *Geochim. Cosmochim. Acta* **62**, 2097–2110.

Oremland, R.S., Stolz, J.F., 2003. The ecology of arsenic. *Science* **300**, 939–944.

Oscarson, D.W., Huang, P.M., Liaw, W.K., 1981a. Role of manganese in the oxidation of arsenite by freshwater lake sediments. *Clay Clay Miner.* **29**, 219–225.

Oscarson, D.W., Huang, P.M., Defosse, D., Herbillion, A., 1981b. Oxidative power of Mn(IV) and Fe(III) oxides with respect to As(III) in terrestrial and aquatic environments. *Nature* **291**, 50–51.

Oscarson, D.W., Huang, P.M., Liaw, W.K., Hammer, U.T., 1983. Kinetics of oxidation of arsenite by various manganese dioxides. *Soil Sci. Soc. Am. J.* **47**, 644–648.

Penn, R.L., Zhu, C., Xu, H., Veblen, D.R., 2001. Iron oxide coatings on sand grains from the Atlantic coastal plain; high-resolution transmission electron microscopy characterization. *Geology* **29**, 843–846.

Pierce, M.L., Moore, C.B., 1980. Adsorption of arsenite on amorphous iron hydroxide from dilute aqueous solution. *Environ. Sci. Technol.* **32**, 344–349.

Poeter, E.P., Hill, M.C., 1998. Documentation of UCODE: A Computer Code for Universal Inverse Modeling, U.S. Geological Survey Water–Resources Investigations Report 98-4080, 116 pp.

Raven, P.R., Jain, A., Loeppert, R.H., 1998. Arsenite and arsenate adsorption on ferrihydrite: Kinetics, equilibrium, and adsorption envelopes. *Environ. Sci. Technol.* **32**, 344–349.

Savoie, J.G., LeBlanc, D.R., 1998. Water-Quality Data and Methods of Analysis for Samples Collected Near a Plume of Sewage-Contaminated Ground Water, Ashumet Valley, Cape Cod, Massachusetts, 1993-94, U.S. Geological Survey Water-Resources Investigations Report 97-4269, 208 pp.

Schreiber, M.E., Simo, J.A., Freiberg, P.G., 2000. Stratigraphic and geochemical controls on naturally occurring arsenic in groundwater, eastern Wisconsin, USA. *Hydrogeol. J.* **8**, 161–176.

Scott, M.J., Morgan, J.J., 1995. Reactions at oxide surfaces. 1. Oxidation of As(III) by synthetic birnessite. *Environ. Sci. Technol.* **29**, 1898–1905.

Seyler, P., Martin, J.-M., 1989. Biogeochemical processes affecting arsenic species distribution in a permanently stratified lake. *Environ. Sci. Technol.* **23**, 1258–1263.

Smedley, P.L., Kinniburgh, D.G., 2002. A review of the source, behavior and distribution of arsenic in natural waters. *Appl. Geochem.* **17**, 517–568.

Smith, R.M., Martell, A.E. (Eds.), 1976. *Critical Stability Constants*, Vol. 4. Plenum Press.

Stadler, S., Jann, S., Höhn, R., Isenbeck-Schröter, M., Niedan, V., Scholz, C., Tretner, A., Davis, J.A., Kent, D.B., 2001. Tracer tests with As(III) in the oxic and suboxic groundwater zones at the USGS Cape Cod site, Mass., USA. In: Cidu, R. (Ed.), *Water–Rock Interaction 2001*. Balkema, Lisse, Italy, pp. 1013–1016.

Stollenwerk, K.G., 1995. Modeling the effects of variable groundwater chemistry on adsorption of molybdate. *Water Resourc. Res.* **31**, 347–357.

Stollenwerk, K.G., 2003. Geochemical processes controlling transport of arsenic in groundwater: a review of adsorption. In: Welch, A.H., Stollenwerk, K.G. (Eds.), *Arsenic in Groundwater*. Kluwer, Norwell, MA, USA, pp. 67–100.

Swartz, C.H., Blute, N.K., Baruzzman, B., Ali, A., Brabander, D., Jay, J., Besancon, J., Islam, S., Hemond, J.F., Harvey, C.F., 2004. Mobility of arsenic in a Bangladesh aquifer: inferences from geochemical profiles, leaching data, and mineralogical characterization. *Geochim. Cosmochim. Acta* **68**, 4539–4557.

Swedlund, P.J., Webster, J.G., 1999. Adsorption and polymerisation of silicic acid on ferrihydrite, and its effect on arsenic adsorption. *Water Resour.* **33**, 3413–3422.

Tani, Y., Miyata, N., Ohashi, M., Ohnuki, T., Seyama, H., Iwahori, K., Soma, M., 2004. Interaction of inorganic arsenic with biogenic manganese oxide produced by a Mn-oxidizing fungus, strain KR21-2. *Environ. Sci. Technol.* **38**, 6618–6624.

Tournassat, C., Charlet, L., Bosbach, D., Manceau, A., 2002. Arsenic(III) oxidation by birnessite and precipitation of manganese(II) arsenate. *Environ. Sci. Technol.* **36**, 493–500.

van Geen, A., Rose, J., Thoral, S., Garnier, J.M., Zheng, Y., Bottero, J.Y., 2004. Decoupling of As and Fe release to Bangladesh groundwater under reducing conditions, Part II.: evidence from sediment incubations. *Geochim. Cosmochim. Acta* **68**, 3475–3486.

Waltham, C.A., Eick, M.J., 2002. Kinetics of arsenic adsorption on goethite in the presence of sorbed silicic acid. *Soil Sci. Soc. Am. J.* **66**, 818–825.

Westall, J.C., Cernik, M., Borkovec, M., 1998. Modeling metal speciation in aquatic systems. In: *Metals in Surface Waters*. Ann Arbor Press, Ann Arbor, MI, pp. 191– 216.

White, A.F., Peterson, M.L., 1996. Reduction of aqueous transition metal species on surfaces of Fe(II)-containing oxides. *Geochim. Cosmochim. Acta* **60**, 3799–3814.

WHO, 1993. *Guidelines for Drinking-Water Quality, vol. 1: Recommendations*, second ed. WHO, Geneva.

Wilkie, J.A., Hering, J.G., 1996. Adsorption of arsenic onto hydrous ferric oxide: effect of adsorbate/adsorbent ratios and co-occurring solutes. *Colloids Surf. A—Physicochem. Eng. Aspects* **107**, 97–110.

Wood, W.W., Kraemer, T.F., Hearn, P.P., 1990. Intragranular diffusion: an important mechanism influencing solute transport in clastic aquifers? *Science* **247**, 1569–1572.

Zapico, M.M., Vales, S., Cherry, J.A., 1987. A wireline piston core barrel for sampling cohesionless sand and gravel below the water table. *Ground Water Monit. Rev.*, 74–82.